



Cite this: *RSC Adv.*, 2017, 7, 55418

# Synthesis of copolyesters with bio-based lauric diacid: structure and physico-mechanical studies

Meiling Chen,<sup>a</sup> Nesren A. H. Saada,<sup>ab</sup> Fei Liu,<sup>id</sup>\*<sup>b</sup> Haining Na<sup>id</sup>\*<sup>b</sup> and Jin Zhu<sup>b</sup>

Lauric diacid (LCDA), also known as 1,12-dodecanedioic acid, is used to develop a series of copolyesters along with 1,4-cyclohexanedicarboxylic acid (CHDA) and 1,4-butanediol (BDO). The resulting poly(butylene lauric dicarboxylate-co-butylene 1,4-cyclohexanedicarboxylate) (PBLC) is proved to be a random copolyester with three triad sequences. When the LCDA content increases from 20 to 60 mol%,  $T_m$  of the copolyester decreases from 133 to 57 °C. At the same time, the tensile modulus and strength decrease from 94 and 14 MPa to 40 and 5 MPa, respectively. Moreover, the elongation at break also drops from 640 to only 50%. However, further increasing the LCDA content to 80 mol%, the copolyester becomes amorphous with no  $T_m$ , and its tensile modulus, strength, and the elongation at break all improve significantly to 68 and 7 MPa, and over 1400%, respectively. More importantly, for the homo-polymer poly(butylene lauric dicarboxylate) (PBL), it has a relatively high  $T_m$  of 73 °C compared to that of polycaprolactone (PCL), but lower tensile modulus and strength, and significantly higher ductility, compared to those of PCL, linear low density polyethylene, and polybutylene succinate.

Received 25th October 2017  
 Accepted 27th November 2017

DOI: 10.1039/c7ra11771j

rsc.li/rsc-advances

## 1 Introduction

Polyesters with linear aliphatic chains have attracted more and more attention from people over the last decades, because they can meet the growing demand in the development of biodegradable and renewable alternatives to non-biodegradable and fossil-based polyesters such as poly(ethylene terephthalate) (PET), and poly(butylene terephthalate) (PBT). Among them, poly(lactic acid) (PLA),<sup>1</sup> poly(butylene succinate) (PBS),<sup>2</sup> and poly(hydroxyalkanoates) (PHAs)<sup>3</sup> have been studied extensively. They have been successfully commercialized and used in many fields such as food packaging, medical devices, 3D printing, and agriculture. These polyesters with linear aliphatic chains typically have ten carbons or less in the backbone, and therefore have low melting points but good biodegradability.<sup>2</sup> On the other hand, other types of polyester with linear aliphatic chains usually have 12 carbons or more. They have structures and properties similar to those of polyethylene because of the low density of the ester functional group.<sup>4</sup> For example, they have higher melting temperatures and hydrophobicities, and better crystallization abilities, which results in decreased biodegradabilities.<sup>4,5</sup>

Likewise, monomers used for the synthesis of long-chain aliphatic polyesters are mostly derived from renewable resources such as fatty acids, *via* biotransformation or chemical

synthetic routes.<sup>4</sup> Monomers with carbon numbers up to 194 have been developed.<sup>6</sup> And polyesters with up to 44  $-\text{CH}_2-$  units between two ester groups have been reported.<sup>7</sup> These results are proof of concept that long-chain linear aliphatic monomers and their correspondent polyester products can be designed and synthesized, so that the gap between semi-crystalline polyolefins and traditional polyesters can be bridged.<sup>8-14</sup>

Of particular interest, long-chain dicarboxylic acids with 12 to 20 carbons have been produced in large scale and are commercially available.<sup>4</sup> Polyesters and polyamides have been synthesized from these monomers.<sup>4</sup> Interestingly, the long-chain dicarboxylic acids with 14 to 20 carbons are building blocks of naturally occurring polyesters such as suberin in cork.<sup>15</sup> However, the one with 12 carbons, namely lauric diacid (LCDA), also known as 1,12-dodecanedioic acid, does not exist in nature. It is therefore a brand new compound created by human beings. Both chemical<sup>16-18</sup> and biological<sup>19,20</sup> methods have been developed for the preparation of LCDA. The chemical synthetic route usually consists of multi-step reactions in order to get cyclic ketones, which subsequently are converted to LCDA *via* oxidation.<sup>16-18</sup> On the other hand, the biological way involves fermentation process using wild type or engineered yeast strains, such as *Candida sorbophila*.<sup>19</sup> Fatty acid or alkane can be used as substrates for this process.<sup>19,20</sup> Nowadays, LCDA has become one of the most widely used monomers for the synthesis of long-chain aliphatic polyesters<sup>21-27</sup> and polyamides.<sup>28,29</sup> It is worth noting that the commercially available LCDA is mainly produced *via* biotransformation from alkane (*i.e.* dodecane) by companies such as Cognis in US, and Cathay Industrial Biothec in China.<sup>4</sup>

<sup>a</sup>College of Food and Pharmacy, Zhejiang Ocean University, Zhoushan, Zhejiang 316000, P. R. China

<sup>b</sup>Key Laboratory of Bio-based Polymeric Materials of Zhejiang Province, Ningbo Institute of Materials Technology and Engineering, Chinese Academy of Sciences, Ningbo, Zhejiang 315201, P. R. China. E-mail: nahaining@nimte.ac.cn; liufei@nimte.ac.cn; Fax: +86-574-86685120; Tel: +86-574-86685120



Polyesters synthesized from LCDA and different diols with an even number of methylene units have melting temperatures ranging from 67 to 90 °C.<sup>30–33</sup> Among them, polyester derived from LCDA and 1,4-butanediol (BDO), namely poly(butylene lauric dicarboxylate) (PBL), has melting point of 74 °C,<sup>24</sup> which is higher than that of poly(butylene adipate) (PBA) (58 °C) and poly(caprolactone) (PCL) (60 °C),<sup>4</sup> but lower than that of PBS (113 °C).<sup>2</sup> Moreover, Celli *et al.* found that PBL has high thermal stability and good crystallization ability, similar to that of polyethylene,<sup>26</sup> but with fairly good biodegradability.<sup>24</sup> Modification on PBL has been performed *via* introduction of aromatic<sup>24</sup> as well as aliphatic ring structure.<sup>34</sup> It was found that incorporation of 70 mol% aromatic ring dramatically hinders the biodegradability of the copolyester,<sup>24</sup> while the same amount of aliphatic ring greatly increases the degradation rate of the copolyester.<sup>34</sup> Since the later one, namely poly(butylene lauric dicarboxylate-*co*-butylene 1,4-cyclohexanedicarboxylate) (PBLC), retains similar biodegradation ability compared to PBL, but has better and tunable properties in a relatively wide range, it is of great importance to reveal the structure–property relationship in this copolyester with different compositions. Therefore, in the current work, we will focus on the sequence distribution and mechanical properties of PBLC, which have not been investigated before. Comparison between PBLC copolyesters and other polyesters with shorter chain as well as polyethylene will be made, in order to provide valuable information to find potential application for the copolyesters.

## 2 Experimental section

### 2.1 Materials

LCDA, BDO, and titanium(IV) butoxide were all purchased from Aladdin Reagent Co., Ltd (Shanghai, China). *trans*-1,4-Cyclohexanedicarboxylic acid (*trans*-CHDA) (99%) was purchased from Nanjing Chemlin Chemical Industry Co., Ltd. Chloroform was obtained from Sinopharm Chemical Reagent Co., Ltd (Shanghai, China). All the chemicals were used as received without further treatment.

### 2.2 Synthesis of PBLC copolyesters

PBLC copolyesters were prepared *via* a two-stage melt polycondensation process involving esterification reaction at 230 °C under N<sub>2</sub>, followed by transesterification reaction at 260 °C under vacuum (Scheme 1). A typical process for the synthesis of PBLC (with 20 mol% of PBL) is described as following. *trans*-CHDA (13.76 g, 0.08 mol, 4 eq.), LCDA (4.60 g, 0.02 mol, 1 eq.), and BDO (14.40 g, 0.16 mol, 8 eq.) were charged to a 250 mL round bottom flask equipped with an overhead mechanical stirrer and distillation device. Ti cat. (1.84 mg, 0.1 wt% of the amount of total diacid) was added to the mixture. The flask was then sealed and applied vacuum (~10 Pa), followed by purging with dry N<sub>2</sub>. This cycle was repeated for three times to remove air and moisture. Subsequently, the flask was heated to 230 °C under N<sub>2</sub> for 3–5 h to finish the esterification reaction. The system was then evacuated to about 1 kPa and simultaneously increased the reaction temperature to 260 °C, and kept for

about half hour to start the second stage, namely the transesterification reaction. It was then placed under vacuum below 20 Pa for about 6 h to remove the extra amount of BDO in order to get high molecular weight products.

Four PBLC copolyesters were synthesized and denoted as PBLC-*x*, where *x* stands for the molar ratio of PBL, which is in the range of 20 to 80 mol%. For example, PBLC-20 means that the polymer contains 20 mol% of PBL. Besides, PBL homopolymer was also synthesized for comparison. All resulted polymers were used without further treatment.

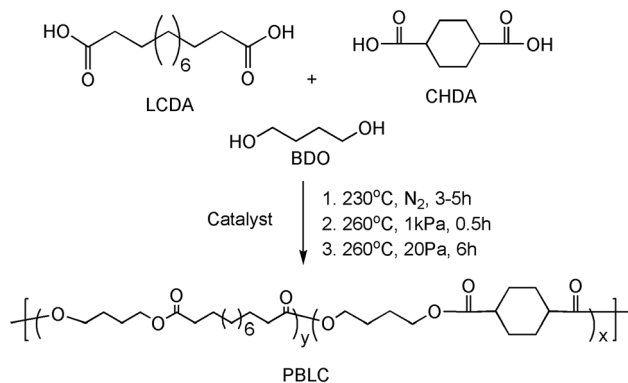
### 2.3 Characterization

**Gel permeation chromatography (GPC).** Number average molecular weights (*M<sub>n</sub>*) and molecular weight distributions (*D<sub>M</sub>*) of PBL, PBC, and PBLC copolyesters were measured on PL-GPC220 gel permeation chromatography (GPC) equipped with a PLgel 5 μm MIXED-D column with a dimension of 300 × 7.5 mm and a refractive index detector. HPLC grade chloroform was used as elution solvent at 40 °C with a flow rate of 1.0 mL min<sup>-1</sup>, and molecular weight was calibrated with polystyrene standard (3070–258 000 g mol<sup>-1</sup>). The concentration of copolyesters was about 6.7 mg mL<sup>-1</sup>.

**Nuclear magnetic resonance (NMR).** The composition and the amount of *trans*-CHDA in the final molecular chains of PBL, PBC, and PBLC copolyesters were determined by <sup>1</sup>H and <sup>13</sup>C NMR in CDCl<sub>3</sub> solvent using a Bruker AVIII400 NMR spectrometer at room temperature.

**X-ray diffraction (XRD).** XRD patterns of PBL, PBC, and PBLC copolyesters were recorded with a Bruker AXS D8 Advance with an X-ray wavelength of 0.1541 nm covering a 2θ range from 5° to 50° within 9 min.

**Differential scanning calorimetry (DSC).** Thermal properties of PBL, PBC, and PBLC copolyesters were characterized using differential scanning calorimeter (METTLER-TOLEDO DSC I). Temperature calibration was carried out using an indium standard. Measurements were performed under a nitrogen atmosphere at a flow rate of 50 mL min<sup>-1</sup>. About 7 mg of sample was placed in an alumina sample pan and the measurement was carried out according to the following process: the sample was heated up to 200 °C at 10 °C min<sup>-1</sup> and held at this temperature for 2 min to erase the heat history. It was then



Scheme 1 Synthesis of PBLC copolyester.



cooled down to  $-30\text{ }^{\circ}\text{C}$  at  $10\text{ }^{\circ}\text{C min}^{-1}$ . Subsequently, a second heating scan was performed at  $10\text{ }^{\circ}\text{C min}^{-1}$  to  $200\text{ }^{\circ}\text{C}$ . The melting point ( $T_m$ ) was obtained from the second heating scan, the crystallization temperature ( $T_c$ ) was obtained from the cooling scan. The degree of crystallinity was calculated according to the following equation:

$$\chi_c(\%) = \frac{\Delta H_m}{f(\text{PBL}) \times \Delta H_m^0(\text{PBL}) + f(\text{trans-PBC}) \times \Delta H_m^0(\text{trans-PBC})} \times 100\%$$

where  $\chi_c$  is the degree of crystallinity,  $f$  is the weight fraction,  $\Delta H_m$  is the experimental melting heat of fusion, and  $\Delta H_m^0$  is the heat of fusion of 100% crystalline ( $170\text{ J g}^{-1}$  for PBL and  $141\text{ J g}^{-1}$  for *trans*-PBC calculated according to the group contribution theory).<sup>35</sup>

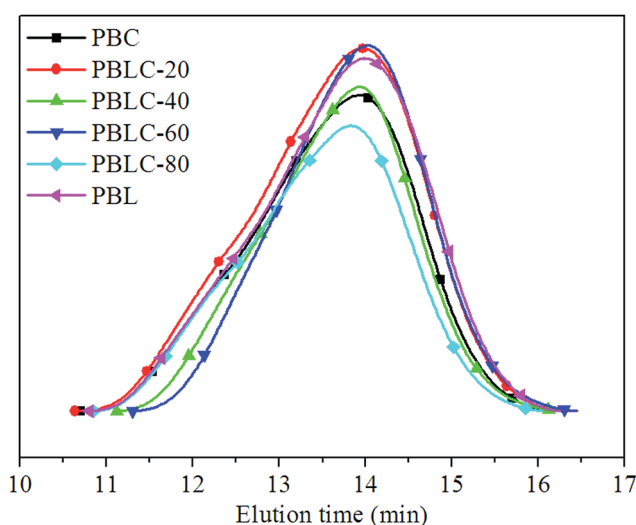


Fig. 1 GPC profiles of PBL, PBC, and PBLC copolyesters.

**Thermal stability.** The thermal stability of PBL, PBC, and PBLC copolyesters were measured using a Mettler-Toledo TGA/DSC thermogravimetric analysis (TGA). 6–10 mg sample was placed in a ceramic furnace and the TGA curve was recorded in a temperature range from  $50\text{ to }800\text{ }^{\circ}\text{C}$  with a heating rate of  $10\text{ }^{\circ}\text{C min}^{-1}$  under dry  $\text{N}_2$  atmosphere with a flow rate of  $50\text{ mL min}^{-1}$ . The temperature at which the weight loss of 5% ( $T_{5\%}$ ) was taken as an index to evaluate the thermal stability of the copolyesters.

**Tensile property.** Tensile testing was performed in an Instron-5567 tensile testing machine with a 500 N load cell. The stretching rate was  $100\text{ mm min}^{-1}$  and the test temperature was  $25\text{ }^{\circ}\text{C}$ . Dumb-bell-shaped sample bars with dimensions of  $35.0\text{ mm}$  (length),  $2.0\text{ mm}$  (neck width) and  $0.5\text{ mm}$  (thickness) were prepared by press-molding at temperature  $20\text{ }^{\circ}\text{C}$  higher than  $T_m$  or  $T_f$  of the sample and subsequently cooled down to temperature below its  $T_c$  or simply to room temperature, without releasing the pressure. All data were obtained by averaging the data from five parallel measurements.

## 3 Results and discussions

### 3.1 Molecular characterization

PBL, PBC, and four PBLC copolyesters with different compositions were successfully obtained. The number average molecular weight ( $M_n$ ) and molecular weight distribution ( $D_M$ ) were determined by GPC analysis. Fig. 1 shows the GPC curves of PBL, PBC, and PBLC copolyesters. Only a single peak was observed centered at elution time of about 14 min, indicating that there is no oligomer in the product. All samples have high  $M_n$  around  $30\text{ }000\text{ g mol}^{-1}$  and  $D_M$  ranging from 1.9 to 2.5.

The molecular structure was analyzed and confirmed by  $^1\text{H}$  NMR spectra. As shown in Fig. 2, all peaks with different chemical shifts are carefully attributed to correspondent protons in PBL, PBC, and a typical copolyester PBLC-20.<sup>34,36</sup> The

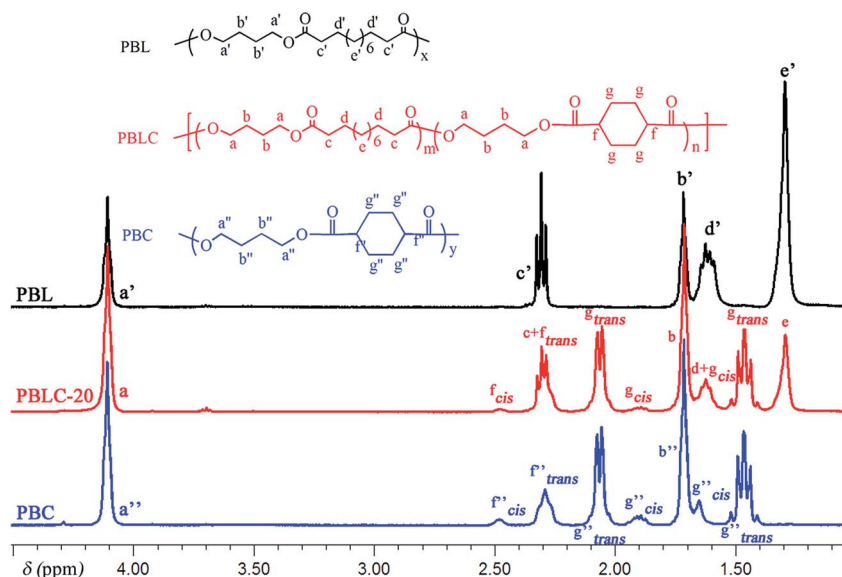


Fig. 2  $^1\text{H}$  NMR (400 MHz,  $\text{CDCl}_3$ ) spectra of PBL, PBC, and PBLC-20.



compositions of the PBLC copolyesters were determined according to the integration ( $I_e$ ,  $I_{g-trans}$ , and  $I_{f-cis}$ ) of three peaks located at  $\delta = 1.294$  ppm (e), 1.466 ppm (*g-trans*), and 2.478 ppm (*f-cis*) (eqn (1)). The molar ratio of *trans*-CHDA isomer in the final products was calculated according to eqn (2), due to the fact that the protons *g* and *f* have different chemical shifts for different CHDA isomers. The correspondent results are listed in Table 1. All samples have PBL molar percentage close to their feed ones. Moreover, the *trans*-CHDA amount of all samples are controlled at around 90 mol%, indicating small amount of isomerization.

$$\text{PBL mol\%} = \frac{I_e}{3I_{g-trans} + 6I_{f-cis} + I_e} \times 100\% \quad (1)$$

$$\text{trans-CHDA mol\%} = \frac{I_{g-trans}}{I_{g-trans} + 2I_{f-cis}} \times 100\% \quad (2)$$

Although the compositions of PBLC copolyesters can be determined easily from  $^1\text{H}$  NMR, the sequence distribution, number-average length of units, and randomness of the copolyesters were unable to obtain according to the  $^1\text{H}$  NMR analysis. Previous studies on a copolyester containing 2,5-furandicarboxylic acid have suggested that the protons of  $-\text{OCH}_2-$  unit in different triads have different chemical shifts resulting from the conjugation effect because of aromatic furan ring.<sup>37</sup> When the aliphatic CHDA is used instead, there is no conjugation effect. Thus the protons of  $-\text{OCH}_2-$  unit in different sequences have the same chemical shift around 4.10 ppm as show in Fig. 2. Similar observation has been reported in the literature before for PBLC as well as poly(butylene adipate-co-butylene 1,4-cyclohexanedicarboxylate) (PBAC).<sup>34,36</sup> However, in the case of PBAC, it was possible to determine the sequence distribution, number-average length of units, as well as randomness from  $^{13}\text{C}$  NMR analysis in a sample with 50 mol% of PBC.<sup>36</sup> Therefore, we performed detailed analysis on the  $^{13}\text{C}$  NMR of PBLC copolyesters in order to find out the sequence distribution of these copolyesters, which has failed to be revealed in a previous study.<sup>34</sup>

We performed  $^{13}\text{C}$  NMR for the four PBLC copolyesters and found that for both PBLC-40 and PBLC-60, there are distinguishable peaks for the chemical shifts in the range of 63.50–63.90 ppm, which could be assigned to different triads sequences in PBLC copolyesters (Fig. 3). The signal in this range is due to the carbons in the butylene unit connected to the ester

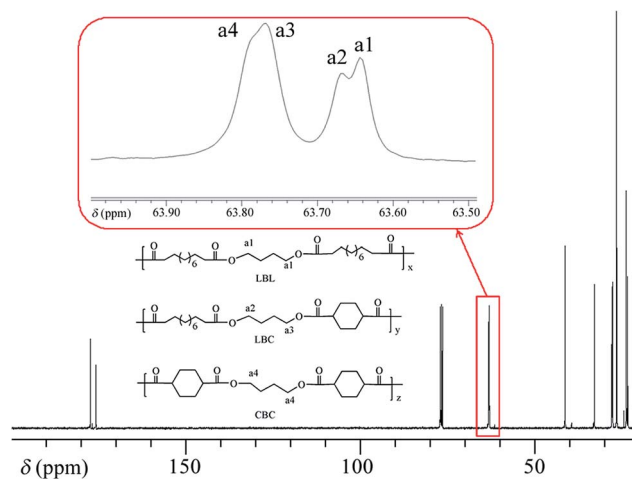


Fig. 3  $^{13}\text{C}$  NMR spectra and triads present in PBLC-40.

bond.<sup>38</sup> From Fig. 3, it can be seen clearly that the three different triads sequences present in the PBLC copolyesters (LBL, LBC, and CBC, see Fig. 3) would result in four different peaks, namely a1, a2, a3, and a4. Their chemical shifts are located at 63.642, 63.669, 63.765, and 63.790 ppm, respectively. The assignment of the peaks to different carbons was based on the fact that the ester bond connected to the aliphatic ring structure has stronger inductive effect than the one connecting to the long aliphatic chain. Therefore, carbon a4 has the highest chemical shift at 63.790 ppm, while carbon a1 has the lowest one at 63.642 ppm.<sup>36,38</sup> By performing a peak fitting on the original curve, four independent peaks can be resolved as displayed in Fig. 4. As a result, the number-average length of BL and BC units ( $L_{\text{BL}}$  and  $L_{\text{BC}}$ ), and randomness ( $R$ ) can be calculated from the integration of the four resolved peaks according to eqn (3)–(5), where  $I_{a1}$ ,  $I_{a2}$ ,  $I_{a3}$ , and  $I_{a4}$  are integration of the four resolved peaks as showed in Fig. 4. The calculated results are summarized in Table 1.

$$L_{\text{BL}} = 1 + \frac{2I_{a1}}{I_{a2} + I_{a3}} \quad (3)$$

$$L_{\text{BC}} = 1 + \frac{2I_{a4}}{I_{a2} + I_{a3}} \quad (4)$$

$$R = \frac{1}{L_{\text{BL}}} + \frac{1}{L_{\text{BC}}} \quad (5)$$

Table 1 Molecular structure of PBL, PBC, and PBLC copolyesters

Sample	$^1\text{H}$ NMR		GPC		$^{13}\text{C}$ NMR		
	PBL (mol%)	<i>trans</i> -CHDA (mol%)	$M_n$ (g mol $^{-1}$ )	$D_M$	$L_{\text{BL}}$	$L_{\text{BC}}$	$R$
PBC	0	88	33 000	2.5	—	—	—
PBLC-20	20	92	34 300	2.2	—	—	—
PBLC-40	38	91	25 500	1.9	1.67	2.24	1.04
PBLC-60	55	89	30 000	2.0	2.66	1.51	1.04
PBLC-80	74	89	29 000	2.4	—	—	—
PBL	100	—	27 400	2.4	—	—	—



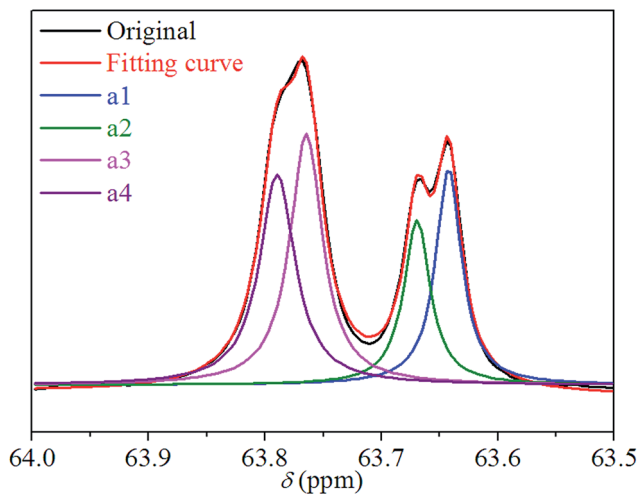


Fig. 4 Peak fitting for chemical shifts of carbons of a1, a2, a3, and a4 in different triads present in PBLC-40.

Both PBLC-40 and PBLC-60 have randomness of 1.04, which is very close to 1, indicating that both of them are random copolyesters. However, since they have different compositions, their unit length are different. PBLC-40 has shorter BL unit length but longer BC unit length than those of PBLC-60. This result is reasonable since PBLC-40 has less amount of BL unit and more amount of BC unit in its molecular chain, compared with that of PBLC-60. For the rest two PBLC copolyesters, namely PBLC-20 and PBLC-80, we were unable to find four distinguishable peaks in the same region. Probably because the signal from the dominate component makes that of the minority one become negligible. Therefore, no further information can be found on the sequence distribution for these two samples. Nevertheless, the results from PBLC-40 and PBLC-60 copolyesters can be used to conclude that PBLC samples are random copolyesters.<sup>34</sup>

### 3.2 Thermal properties and crystal structure

The thermal properties including melting temperature ( $T_m$ ), crystallization temperature ( $T_c$ ), and thermal stability of PBL, PBC, and PBLC copolyesters were investigated by using DSC and TGA analysis.

Fig. 5 shows the DSC curves of these samples in the second heating, and cooling scans. Table 2 collects the relevant thermal data. In the first place, from Fig. 5 we can see that both PBL and PBC homo-polymers are able to crystallize, and show strong and sharp peaks in the second heating and cooling scans. PBL has  $T_m$  of 73 °C,  $T_c$  of 54 °C, melting enthalpy ( $\Delta H_m$ ) of 7 J g<sup>-1</sup> and degree of crystallinity ( $\chi_c$ ) of 4.0%. All these values are lower than those of PBC. Especially, the low  $\chi_c$  of PBL indicates that it has weaker crystallization ability compared to that of PBC. Comparing with other linear aliphatic polyesters derived from BDO and dicarboxylic acids with different carbon numbers, PBL has higher  $T_m$  than those with shorter chain length in the dicarboxylic acids, except for succinic acid (PBS,  $T_m$  113 °C) and ethanedioic acid (PBE,  $T_m$  105 °C), and lower  $T_m$  than those with

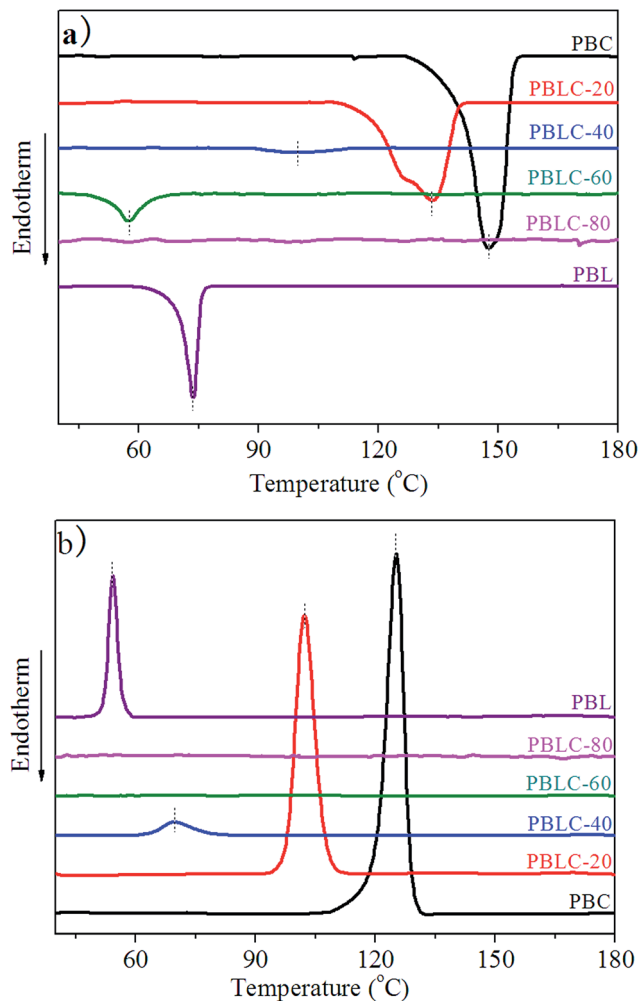


Fig. 5 DSC curves for PBL, PBC, and PBLC copolyesters: (a) second heating and (b) cooling scans.

Table 2 Thermal properties of PBL, PBC, and PBLC copolyesters<sup>a</sup>

Sample	$T_m$ (°C)	$\Delta H_m$ (J g <sup>-1</sup> )	$T_c$ (°C)	$\chi_c$ (%)	$T_{5\%}$ (N <sub>2</sub> ) (°C)	$T_{d,max}$ (N <sub>2</sub> ) (°C)
PBC	147	24	125	19.3	382	409
PBLC-20	133	17	103	12.2	371	408
PBLC-40	98	1	70	0.7	373	412
PBLC-60	57	2.5	—	1.6	378	412
PBLC-80	—	—	—	—	380	415
PBL	73	7	54	4.0	375	417

<sup>a</sup> Melting temperature  $T_m$ , melting enthalpy  $\Delta H_m$  and degree of crystallinity  $\chi_c$  are determined from second heating scan of DSC curves and the crystallization temperature  $T_c$  is determined from the cooling scans of DSC curves, the temperature at 5% weight loss  $T_{5\%}$  is determined by TGA in N<sub>2</sub> atmosphere.

longer chain length in the dicarboxylic acids.<sup>4</sup> In the second place, for the rest four PBLC copolyesters, both  $T_m$  and  $T_c$  decrease steadily with the increasing of BL content. In addition, both  $\Delta H_m$  and  $\chi_c$  decrease to fairly small value, indicating poor crystallization ability. As we can see from Fig. 5 that melting



peaks become broad and weak. When BL content is 80 mol%, namely PBLC-80, the copolyester shows neither melting nor crystallization peak in the DSC curves. Therefore, from the DSC analysis, PBLC-80 is an amorphous copolyester. For PBLC-60 on the other hand, it shows a very small peak in the second heating scan but no peak in the cooling scan, indicating fairly poor crystallization ability, compared with other copolyesters and the homo-polymers.

Fig. 6 shows the TGA curves of PBL and PBLC copolyesters, the related data are collected in Table 2. PBL has slightly lower  $T_{5\%}$  but higher  $T_{d,max}$  than those of PBC. Moreover, for the four PBLC copolyesters, both  $T_{5\%}$  and  $T_{d,max}$  increase gradually with the increasing of BL content, indicating increased thermal stability. Nonetheless, all samples have high thermal resistance with  $T_{5\%}$  and  $T_{d,max}$  over 370 and 405 °C, respectively. As a result, these materials can be processed safely without thermal degradation at temperatures 30–50 °C higher than their corresponding  $T_m$ .

The crystalline structure of PBL, PBC, and PBLC copolyesters was studied by using X-ray diffraction (XRD). The XRD patterns displayed in Fig. 7 clearly indicate that PBL and PBC homopolymers have totally different crystalline structure. The crystal lattice of PBC is of triclinic type,<sup>36</sup> with diffraction peaks at  $2\theta = 15.16, 16.34, 18.24, 19.64, 20.59,$  and  $22.53^\circ$ . On the other hand, PBL is of the orthorhombic type similar to that of polyethylene,<sup>4,26</sup> with diffraction peaks at  $2\theta = 21.39,$  and  $23.72^\circ$ . For the other four PBLC copolyesters, their crystalline structure can be divided into two groups. For PBLC-20, 40, and 60, they are the triclinic type similar to that of PBC. For PBLC-80, it is the orthorhombic type similar to that of PBL.<sup>39</sup>

For the first group, with increasing amount of BL unit, the intensity of the diffraction peaks becomes weak, and the peak at  $2\theta = 19.64^\circ$  disappears. This observation is similar to what has been reported in a PBAC copolymer series.<sup>36</sup> Therefore, this result suggests that the crystalline phase in this group of PBLC copolyesters is the PBC crystalline phase.<sup>39</sup> Incorporation of BL unit hinders the crystallization of BC unit, and only small amount of BC unit is able to organize into crystalline phase.

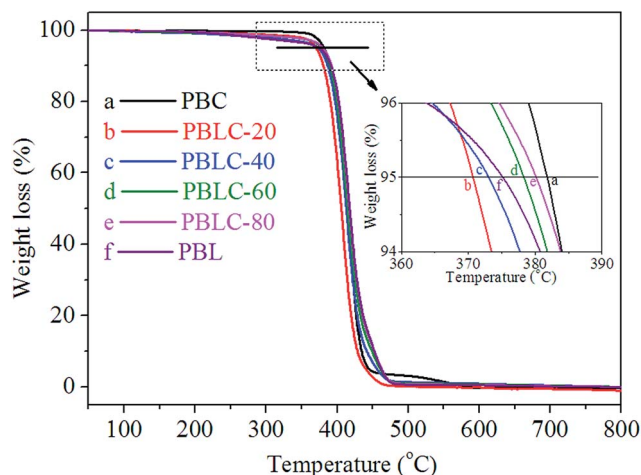


Fig. 6 TGA curves for PBC, PBL, and PBLC copolyesters.

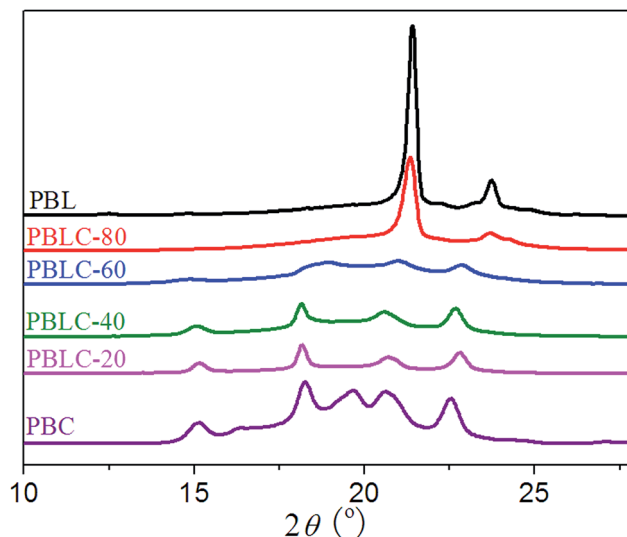


Fig. 7 X-ray diffraction (XRD) patterns of PBL, PBC, and PBLC copolyesters.

This explains the fact that this group of PBLC copolyesters have very low heat of fusion and degree of crystallinity, as showed in Table 2. Moreover, the BL unit is in the amorphous region.

Based on these results, it is reasonable to imply that the decreasing of  $T_m$  from 133 to 57 °C for the first group of PBLC copolyesters is due to the depression effect of the non-crystalline BL unit on the BC unit. This depression effect can be quantitatively described by the Flory equation.<sup>40</sup> The Flory equation deals with the relationship between the  $T_m$  of the PBLC copolyester ( $T_{m,PBLC}$ ) and the equilibrium  $T_m$  of the PBC homo-polymer ( $T_{m,PBC}^\circ$ ), as showed in eqn (6):

$$\frac{1}{T_{m,PBLC}} = \left( \frac{R}{\Delta H_u} \right) \ln p + \frac{1}{T_{m,PBC}^\circ} \quad (6)$$

where  $R$  is the universal gas constant,  $p$  is the molar fraction of the crystallizable BC unit, and  $\Delta H_u$  is the enthalpy of fusion per crystallizable repeating BC unit. According to our previous finding, the crystallizable BC unit is formed merely from the *trans*-CHDA isomer, therefore,  $p$  is the molar fraction of *trans*-BC unit.<sup>36</sup> By using the Flory equation, we find a perfect linear relationship between  $\ln p$  and  $1/T_{m,PBLC}$ , for the first group of PBLC copolyesters, as showed in Fig. 8. The correlation coefficient ( $R^2$ ) for the linear fitting is 0.999. Therefore, it can be concluded that when the BL content is lower than 60 mol%, the random PBLC copolyesters have decreased  $T_m$  due to the depression effect of the non-crystalline BL unit on the crystallizable *trans*-BC unit.

### 3.3 Mechanical properties

The mechanical properties of PBL and PBLC copolyesters were characterized by tensile testing. The representative tensile strain–stress curves are showed in Fig. 9, and the mechanical properties data are listed in Table 3. In the first place, for the two homo-polymers, PBL has very similar tensile modulus, but higher tensile strength and elongation at break compared to



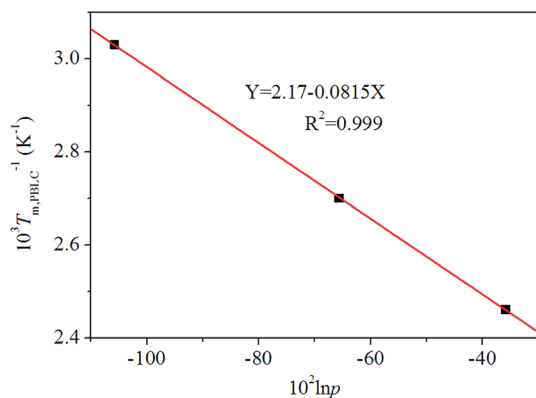


Fig. 8 Plot of Flory equation (black squares) and linear fitting (red line) for the first group of PBLC copolyesters.

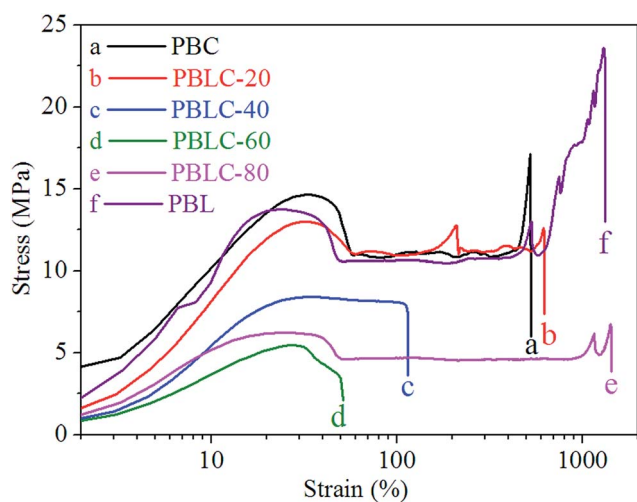


Fig. 9 Representative tensile strain–stress curves of PBL and PBLC copolyesters.

Table 3 Mechanical properties of PBL and PBLC copolyesters<sup>a</sup>

Sample	$E$ (Mpa)	$\sigma_t$ (Mpa)	$\epsilon_b$ (%)	$\sigma_y$ (Mpa)	$\epsilon_y$ (%)
PBC	157 ± 7	17.0 ± 1.0	520 ± 7	14.0 ± 1.0	21.0 ± 1.0
PBLC-20	94 ± 8	14.0 ± 2.0	640 ± 27	12.0 ± 1.0	26.0 ± 1.0
PBLC-40	62 ± 5	8.0 ± 0.4	100 ± 14	—	—
PBLC-60	40 ± 2	5.0 ± 0.2	50 ± 3	—	—
PBLC-80	68 ± 3	7.0 ± 1.0	1431 ± 16	7.0 ± 0.5	29.0 ± 0.2
PBL	141 ± 20	23.0 ± 0.4	1354 ± 16	13.0 ± 0.3	28.0 ± 0.1

<sup>a</sup> Tensile modulus  $E$ , tensile strength  $\sigma_t$ , elongation at break  $\epsilon_b$ , yield stress  $\sigma_y$  and yield strain  $\epsilon_y$  are determined by tensile testing.

those of PBC.<sup>41</sup> However, replacing BDO with 1,5-pentanediol, the resulted polyester PPeDo has tensile modulus of 344 MPa, which is significantly higher than that of PBL.<sup>42</sup> Moreover, compared with some other polymers such as linear low density polyethylene (LLDPE), PBS, and PCL, PBL also has smaller modulus but higher elongation at break,<sup>42,43</sup> probably because PBL has relatively low degree of crystallinity than those of the

above mentioned polymers.<sup>42</sup> In the second place, as showed in Fig. 10 and 11, when 20 mol% of a second unit is introduced to the homo-polymer, both PBLC-20 and PBLC-80 have largely decreased tensile modulus and strength, but slightly increased elongation at break, compared with those of PBC and PBL, respectively. This phenomenon is due to the fact that the introduction of the second units (*i.e.* BL or BC) breaks the crystalline of the homo-polymer. If we consider the two homo-polymers as rigid and tough materials, these two copolyesters can be considered as soft but tough materials. However, further increasing the amount of the second unit to 40 mol%, both PBLC-40 and PBLC-60 have further decreased tensile modulus and strength, and significantly decreased elongation at break. Moreover, both copolyesters break before they yield, therefore, no yield strength or strain can be observed. As a result, these two copolyesters are soft and brittle. In another word, increasing the amount of one unit from 0 to 50 mol%, namely decreasing the content of the other one from 100 to 50 mol%, the PBLC copolyester experiences a ductile-to-brittle transition.

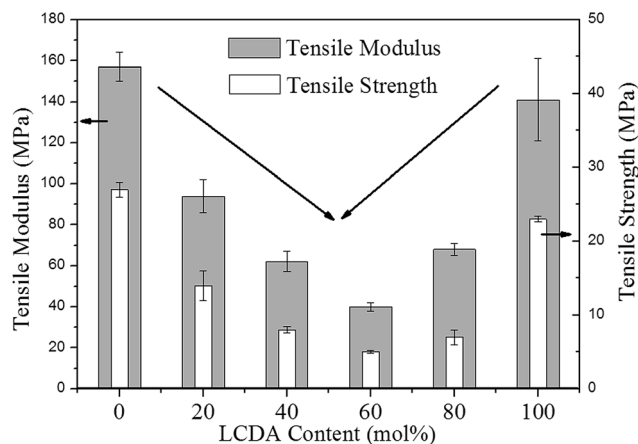


Fig. 10 Trends of tensile modulus and strength with different LCDA content.

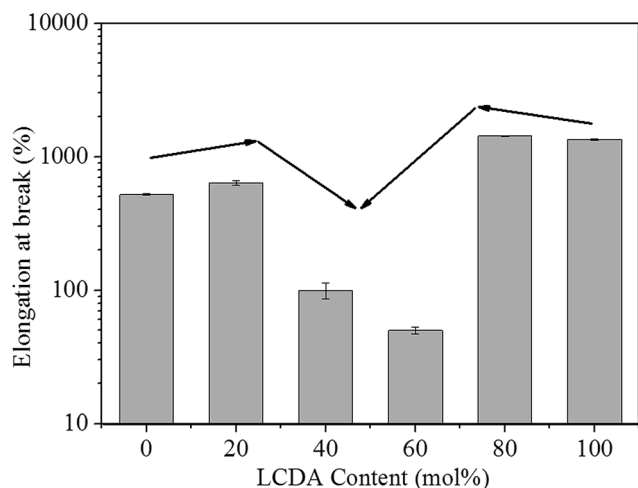


Fig. 11 Trends of elongation at break with different LCDA content.



This transition is very different from other copolyesters series, in which the elongation at break of the copolyester with composition near 50/50 is usually the highest.<sup>43,44</sup> A possible explanation to this phenomenon is due to the low  $M_n$  and possible high entanglement molecular weight for PBLC-40 and PBLC-60, in which the molecular chain can not form effective entanglements that are necessary for good ductility.<sup>45</sup>

## 4 Conclusion

In conclusion, we have developed a series of copolyesters from a bio-based long chain dicarboxylic acid and an aliphatic ring structure. The copolyesters with different compositions have very different structure and properties compared with their parenting homo-polymers. It was found that the copolyester is a random copolymer with three triad sequences according to the <sup>13</sup>C NMR analysis. The copolyester with increasing amount of BL unit to 60 mol% tends to have decreased  $T_m$  as well as  $T_c$ , compared with those of the PBC homo-polymer. This is because the BL unit would form defect in the PBC crystalline region as proved by applying the Flory equation. Moreover, these copolyesters have the same crystalline lattice type to PBC. However, further increasing the BL unit to 80 mol% in the copolyester, it becomes amorphous as showed in DSC scans, and its XRD pattern is similar to that of PBL. For the first time the mechanical properties of the copolyesters are revealed. It was found that when the composition is getting close to 50/50, the tensile modulus and strength decrease gradually, but surprisingly, the elongation at break also drops sharply, compared with the two homo-polymers. In addition, for the homo-polymer PBL, although the tensile modulus is relatively low, it has better ductility compared to polymers like LLDPE, PBS, and PCL.

## Conflicts of interest

There are no conflicts to declare.

## Acknowledgements

The authors are grateful for the financial support by the Zhejiang Provincial Natural Science Foundation (ZJNSF, LQ15C200010), National Natural Science Foundation of China (NSFC, 51503217), Zhejiang Province Public Welfare Project (2017C31081) and Open Project Program of MOE Key Laboratory of Macromolecular Synthesis and Functionalization, Zhejiang University(2016MSF001).

## References

- 1 K. Madhavan Nampoothiri, N. R. Nair and R. P. John, *Bioresour. Technol.*, 2010, **101**, 8493–8501.
- 2 J. Xu and B. H. Guo, *Biotechnol. J.*, 2010, **5**, 1149–1163.
- 3 G.-Q. Chen, *Chem. Soc. Rev.*, 2009, **38**, 2434–2446.
- 4 F. Stempfle, P. Ortmann and S. Mecking, *Chem. Rev.*, 2016, **116**, 4597–4641.
- 5 X. Y. Lee, M. U. Wahit and N. Adrus, *J. Appl. Polym. Sci.*, 2016, **133**, 1–9.
- 6 F. Ian, F. Jens and I. Hiriyakkanavar, *J. Chem. Soc., Perkin Trans. 1*, 1998, 1229–1235.
- 7 C. L. F. De Ten Hove, J. Penelle, D. A. Ivanov and A. M. Jonas, *Nat. Mater.*, 2004, **3**, 33–37.
- 8 F. Stempfle, D. Quinzler, I. Heckler and S. Mecking, *Macromolecules*, 2011, **44**, 4159–4166.
- 9 C. Vilela, A. J. D. Silvestre and M. A. R. Meier, *Macromol. Chem. Phys.*, 2012, **213**, 2220–2227.
- 10 S. Huf, S. Krügener, T. Hirth, S. Rupp and S. Zibek, *Eur. J. Lipid Sci. Technol.*, 2011, **113**, 548–561.
- 11 A. Pascual, H. Sardon, A. Veloso, F. Ruipérez and D. Mecerreyes, *ACS Macro Lett.*, 2014, **3**, 849–853.
- 12 M. P. F. Pepels, M. R. Hansen, H. Goossens and R. Duchateau, *Macromolecules*, 2013, **46**, 7668–7677.
- 13 A. Díaz, R. Katsarava and J. Puiggalí, *Int. J. Mol. Sci.*, 2014, **15**, 7064–7123.
- 14 Z. S. Petrović, J. Milić, Y. Xu and I. Cvetković, *Macromolecules*, 2010, **43**, 4120–4125.
- 15 P. E. Kolattukudy, *Science*, 1980, **208**, 990–1000.
- 16 K. Osowska-Pacewicka and H. Alper, *J. Org. Chem.*, 1988, **53**, 808–810.
- 17 C.-M. Che, W.-P. Yip and W.-Y. Yu, *Chem.-Asian J.*, 2006, **1**, 453–458.
- 18 P. P. Thottumkara and T. K. Vinod, *Org. Lett.*, 2010, **12**, 5640–5643.
- 19 H. Lee, Y. E. C. Sugiharto, S. Lee, G. Park, C. Han, H. Jang, W. Jeon, H. Park, J. Ahn, K. Kang and H. Lee, *Appl. Microbiol. Biotechnol.*, 2017, 1–10.
- 20 W. Cao, H. Li, J. Luo, J. Yin and Y. Wan, *J. Ind. Microbiol. Biotechnol.*, 2017, **44**, 1191–1202.
- 21 X. Kong, H. Qi and J. M. Curtis, *J. Appl. Polym. Sci.*, 2014, **131**, 4–10.
- 22 D. G. Barrett, W. Luo and M. N. Yousaf, *Polym. Chem.*, 2010, **1**, 296.
- 23 F. Migneco, Y. C. Huang, R. K. Birla and S. J. Hollister, *Biomaterials*, 2009, **30**, 6479–6484.
- 24 C. Berti, A. Celli, P. Marchese, G. Barbiroli, F. Di Credico, V. Verney and S. Commereuc, *Eur. Polym. J.*, 2008, **44**, 3650–3661.
- 25 C. Berti, A. Celli, P. Marchese, E. Marianucci, G. Barbiroli and F. Di Credico, *e-Polym.*, 2007, **7**, 1–18.
- 26 A. Celli, G. Barbiroli, C. Berti, D. C. Francesco, C. Lorenzetti, P. Marchese and E. Marianucci, *J. Polym. Sci. Part B Polym. Phys.*, 2007, **45**, 1053–1067.
- 27 A. Takasu, A. Takemoto and T. Hirabayashi, *Biomacromolecules*, 2006, **7**, 6–9.
- 28 H. W. Starkweather Jr, P. Avakian, K. H. Gardner, B. S. Hsiao, M. Y. Keating and H. Ng, *J. Therm. Anal. Calorim.*, 2000, **59**, 519–530.
- 29 X. Cui and D. Yan, *Eur. Polym. J.*, 2005, **41**, 863–870.
- 30 E. M. Woo, J. W. Barlow and D. R. Paul, *Polymer*, 1985, **26**, 763–773.
- 31 U. Witt, R.-J. Müller, J. Augusta, H. Widdecke and W.-D. Deckwer, *Macromol. Chem. Phys.*, 1994, **195**, 793–802.



- 32 A. Almontassir, S. Gestí, L. Franco and J. Puiggali, *Macromolecules*, 2004, **37**, 5300–5309.
- 33 G. Barbiroli, C. Lorenzetti, C. Berti, M. Fiorini and P. Manaresi, *Eur. Polym. J.*, 2003, **39**, 655–661.
- 34 C. Berti, A. Celli, P. Marchese, G. Barbiroli, F. Di Credico, V. Verney and S. Commereuc, *Eur. Polym. J.*, 2009, **45**, 2402–2412.
- 35 K. G. Joback and R. C. Reid, *Chem. Eng. Commun.*, 1987, **57**, 233–243.
- 36 F. Liu, J. Qiu, J. Wang, J. Zhang, H. Na and J. Zhu, *RSC Adv.*, 2016, **6**, 65889–65897.
- 37 B. Wu, Y. Xu, Z. Bu, L. Wu, B.-G. Li and P. Dubois, *Polymer*, 2014, **55**, 3648–3655.
- 38 T. Debuissy, E. Pollet and L. Avérous, *J. Polym. Sci., Part A: Polym. Chem.*, 2017, 2738–2748.
- 39 C. Berti, A. Celli, P. Marchese, E. Marianucci, S. Sullalti and G. Barbiroli, *Macromol. Chem. Phys.*, 2010, **211**, 1559–1571.
- 40 M. Yokouchi, Y. Sakakibara, Y. Chatani, H. Tadokoro and T. Tanaka, *Macromolecules*, 1975, **9**, 266–273.
- 41 F. Liu, J. Zhang, J. Wang, X. Liu, R. Zhang, G. Hu, H. Na and J. Zhu, *J. Mater. Chem. A*, 2015, **3**, 13637–13641.
- 42 J. Lu, L. Wu and B. G. Li, *ACS Sustainable Chem. Eng.*, 2017, **5**, 6159–6166.
- 43 X. Dai and Z. Qiu, *Polym. Degrad. Stab.*, 2016, **134**, 305–310.
- 44 A. Celli, P. Marchese, S. Sullalti, J. Cai and R. A. Gross, *Polymer*, 2013, **54**, 3774–3783.
- 45 G. Stoclet, G. Gobius du Sart, B. Yeniad, S. de Vos and J. M. Lefebvre, *Polymer*, 2015, **72**, 165–176.

